Novel Trisubstituted Benzimidazoles, Targeting *Mtb* FtsZ, as a New Class of Antitubercular Agents

Kunal Kumar,[†] Divya Awasthi,[†] Seung-Yub Lee,[‡] Ilaria Zanardi,[‡] Bela Ruzsicska,[‡] Susan Knudson,[§] Peter J. Tonge,[†,‡] Richard A. Slayden,[§] and Iwao Ojima*,[†,‡]

[†]*Department of Chemistry, and* [‡]*Institute of Chemical Biology and Drug Discovery, State University of New York at Stony Brook, Stony Brook, New York 11794-3400, United States, and* [§]*Department of Microbiology, Immunology and Pathology, Colorado State University, Fort Collins, Colorado 80523-1682, United States*

Libraries of novel trisubstituted benzimidazoles were created through rational drug design. A good number of these benzimidazoles exhibited promising MIC values in the range of $0.5-6\,\mu g/mL$ ($2-15\,\mu M$) for their antibacterial activity against *Mtb* H37Rv strain. Moreover, five of the lead compounds also exhibited excellent activity against clinical *Mtb* strains with different drug-resistance profiles. All lead compounds did not show appreciable cytotoxicity ($IC_{50} > 200\,\mu M$) against Vero cells, which inhibited *Mtb* FtsZ assembly in a dose dependent manner. The two lead compounds unexpectedly showed enhancement of the GTPase activity of *Mtb* FtsZ. The result strongly suggests that the increased GTPase activity destabilizes FtsZ assembly, leading to efficient inhibition of FtsZ polymerization and filament formation. The TEM and SEM analyses of *Mtb* FtsZ and *Mtb* cells, respectively, treated with a lead compound strongly suggest that lead benzimidazoles have a novel mechanism of action on the inhibition of *Mtb* FtsZ assembly and Z-ring formation.

Introduction

Tuberculosis (TB[a]) is one of the leading infectious diseases and remains a major global health problem. According to WHO, 9.2 million new cases and 1.7 million deaths from TB have been reported.[1] With the emergence of HIV, TB has become the most common opportunistic infection afflicting patients living with AIDS. There are 0.7 million HIV-positive people infected with TB, contributing to 0.2 million deaths worldwide.[1] The lethal combination of TB and HIV is fueling the TB epidemic in many parts of the world, especially Africa.[1] Poor chemotherapeutics and the inadequate administration of drugs have led to the development of multidrug resistant TB (MDR-TB),[2] the treatment of which requires administration of more expensive, second line antibiotics for up to 2 years. In addition, even more alarming cases of extensively drug resistant strains of TB (XDR-TB) that are resistant to both first and second line drugs have been reported.[3] Recent findings by WHO from 2000 to 2004 suggested that 4% of MDR-TB cases meet the criteria for XDR-TB. Consequently, there is a pressing need for the development of novel TB drugs that are effective against both drug sensitive and resistant *Mtb* strains.

FtsZ, a tubulin homologue, is a highly conserved and ubiquitous bacterial cell division protein. Similar to the process of microtubule formation by tubulin, FtsZ polymerizes in a GTP-dependent manner, forming a highly dynamic cytokinetic structure, designated as the Z-ring, at the midpoint of the cell.[4,5] The recruitment of the other cell division proteins leads to Z-ring contraction, resulting in septum formation. Because of the requirement of FtsZ in mycobacterial cytokinesis, inhibition of FtsZ is a promising target for antituberculosis drug discovery.[6−9] While tubulin and FtsZ share structural and functional homology and tubulin inhibitors are known to affect FtsZ assembly,[6−8] the limited sequence homology at the protein level affords an opportunity to discover FtsZ-specific compounds with limited cytotoxicity to eukaryotic cells.[10] Since FtsZ is a novel drug target, compounds targeting FtsZ are expected to be active against drug resistant *Mtb* strains.[11] Furthermore, the validation of FtsZ as a novel antibacterial drug target has been confirmed by the work of various groups including ours.[12−24]

Researchers at the Southern Research Institute screened known tubulin inhibitors against *Mtb* and identified several pyridopyrazine and pteridine based FtsZ inhibitors with anti-TB activity.[12−14] Later, Slayden et al. found that thiabendazole and albendazole, known tubulin inhibitors, interfered and delayed the *Mtb* cell division processes.[8] Taking into account the structural similarity of the pyridopyrazine moiety, pteridine moiety, albendazole, and thiabendazole,[12−14] we envisioned that the benzimidazole scaffold would be a good starting point for the development of novel FtsZ inhibitors, which will have activity against both drug sensitive and drug resistant *Mtb*. Therefore, trisubstituted benzimidazoles were investigated for antibacterial activity. Specifically we report

---

*To whom correspondences should be addressed. Phone: 631-632-1339. Fax: 631-632-7942. E-mail: iojima@notes.cc.sunysb.edu.

[a] Abbreviations: ACN, acetonitrile; AIDS, acquired immuno deficiency syndrome; BCA, bicinchoninic acid; DIPEA, diisopropyl ethylamine; DMF, *N,N*-dimethylformamide; DMSO, dimethylsulfoxide; *E. coli, Escherichia coli*; FtsZ, filamenting temperature sensitive mutant Z; GTP, guanosine triphosphate; GTPase, guanosine triphosphatase; HIV, human immunodeficiency virus; MABA, microplate Alamar Blue assay; MDR-TB, multidrug resistant tuberculosis; MIC, minimum inhibitory concentration; *Mtb, Mycobacterium tuberculosis*; OADC, oleic acid/albumin/catalase ; /catalase ; PBS, phosphate buffered saline; Pi, inorganic phosphate; RT, room temperature; SAR, structure−activity relationship; SEM, scanning electron microscopy; TB, tuberculosis; TEM, transmission electron microscopy; THF, tetrahydrofuran; TLC, thin layer chromatography; WHO, World Health Organization; XDR-TB, extremely drug resistant tuberculosis.
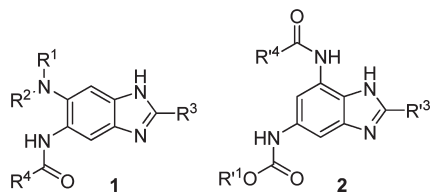
Figure 1. Proposed 2,5,6- and 2,5,7-trisubstituted benzimidazoles.

Scheme 1. Synthesis of 2,5,6-Trisubstituted Benzimidazoles[a]
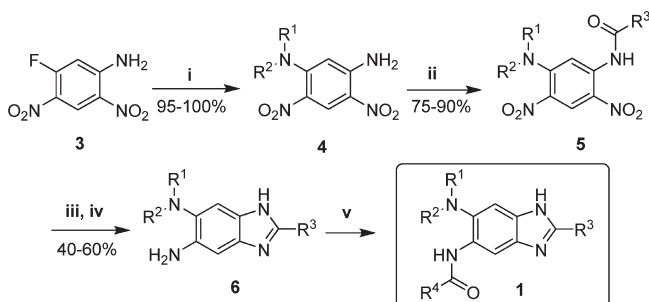
[a] Reagents and conditions: (i) Et_2NH, DIPEA, THF, 2 h, room temperature (RT); (ii) R^3COCl, pyridine, reflux, overnight; (iii) 10% Pd/C—HCO_2NH_4, dioxane, EtOH, 1 h, RT; (iv) 4 N HCl, reflux, 4 h; (v) (a) R^4COCl or R^4COOCl, CH_2Cl_2, overnight, RT; (b) aminomethylated polystyrene resin, CH_2Cl_2, overnight, RT.

Scheme 2. Synthesis of 2,5,7-Trisubstituted Benzimidazoles[a]

[a] Reagents and conditions: (i) 6 N HCl, reflux, 1.5 days; (ii) $SOCl_2$, reflux, overnight; (iii) NaN_3, acetone, 0 °C, 30 min; (iv) toluene, reflux, 4 h; (v) R'^1OH, RT, 1 day; (vi) 10% Pd/C—HCO_2NH_4, EtOH, 1 h, RT; (vii) $R'^2CH(OH)SO_3Na$, $EtOH/H_2O$ (1:1); (viii) (a) R'^3COCl or R'^3OCOCl, DMF, overnight, RT; (b) aminomethylated polystyrene resin, DMF, overnight, RT.
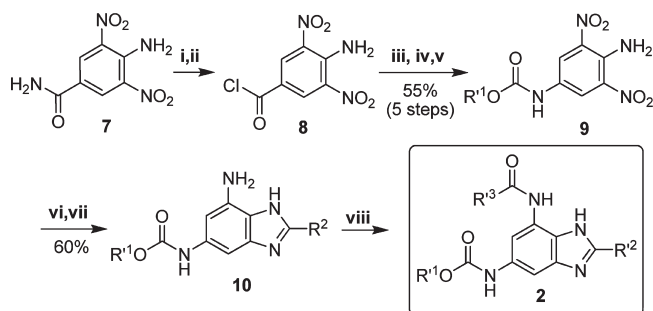
the activity of 2,5,6- and 2,5,7-trisubstituted benzimidazoles against *Mtb* (Figure 1). Importantly, this work substantiates trisubstituted benzimidazoles for the development of next generation antimycobacterial inhibitors with activity against difficult to treat clinical strains.

Chemistry

The 2,5,6-trisubstituted benzimidazoles were synthesized as outlined in Scheme 1. The aromatic nucleophilic substitution of commercially available 2,4-dinitro-5-fluoroaniline (**3**) with diethylamine afforded 5-diethylaminodinitroaniline **4a** ($R^1 = R^2 = Et$) in quantitative yield. The acylation of **4a** with different acyl chlorides afforded the corresponding *N*-acylanilines **5a-1**–**8** in 75–90% yields. The reduction and subsequent acid-catalyzed cyclization gave 5-aminobenzimidazoles **6a-1**–**8** in 40–60% yield. The advanced intermediates **6a-1**–**8** were dissolved in dichloromethane and transferred to a 96-well plate. Subsequently, 33 different acyl chlorides and/or alkyl chloroformates were added to **6a-1**–**8** and reacted at room temperature overnight using a shaker. To the reaction mixture was added an aminomethylated polystyrene resin to scavenge excess or unreacted acyl chlorides and/or alkyl chloroformates. After the mixture was reacted overnight with gentle shaking, the resin was filtered to afford a library of 272 2,5,6-trisubstituted benzimidazoles **1a** ($R^1 = R^2 = Et$) with good to high purity based on LC—MS/UV analysis (see the Supporting Information for the detailed experimental procedures, structures of intermediates, and library).

The 2,5,7-trisubstituted benzimidazoles were synthesized as outlined in Scheme 2. Commercially available 5-amino-2,4-dinitrobenzamide (**7**) was hydrolyzed to give 4-amino-3,5-dinitrobenzoic acid, which was converted to acyl chloride **8**. The reaction of **8** with sodium azide afforded the corresponding acyl azide, which was subjected to the Curtius rearrangement to give the corresponding isocyanate. The isocyanate was subsequently reacted with methanol or ethanol to give the

corresponding carbamates **9a** (R'^1 = Et) or **9b** (R'^1 = Me) in 78–85% yield (for five steps) as a bright red solid. The reduction of **9a,b** followed by cyclocondensation with the bisulfite salts of different aldehydes afforded 7-aminobenzimidazoles **10a-A**–**F** and **10b**. The final acylation of **10a,b** in the same manner as that for the library of **1a** gave the 77-compound library of 2,5,7-trisubstituted benzimidazoles **2** with good to high purity (see the Supporting Information for the detailed experimental procedures, structures of intermediates, and library).

Results and Discussion

The libraries of 2,5,6- and 2,5,7-trisubstituted benzimidazoles **1a** and **2** (349 compounds) were screened for their activity against *Mtb* H37Rv using the "microplate Alamar Blue assay (MABA)"[25] in a 96-well format (single point assay in triplicates). Of these, 26 compounds were identified to inhibit the growth of *Mtb* H37Rv with MIC values of ≤5 μg/mL. Furthermore, among the 26 hits, the resynthesized pure 9 compounds showed MIC values of 0.50–6.1 μg/mL (1.5–15 μM) (Table 1).

Preliminary structure—activity relationship studies of hits from the library of **1a** indicated that cyclohexyl and diethylamino groups at the 2 and 6 positions, respectively, were critically important for antibacterial activity (Figure 2). Accordingly, another library of **1** (**1-G**: 238 compounds) was synthesized with different dialkylamino substituents at the 6-position but retaining the cyclohexyl group at the 2-position using the procedures similar to those for the synthesis of the libraries of **1a** (Scheme 1). (See Supporting Information for the detailed experimental procedures, structures of the intermediates, and library.)

On the basis of the MABA screening (single point assay in triplicates), 54 compounds were identified as hits, which inhibited the cell growth with MIC values of 5 μg/mL or less. Among the 54 hits, resynthesized pure **1b-G1** and **1b-G2** showed MIC values of 0.39 μg/mL (1.0 μM) and 1.56 μg/mL (3.7 μM), respectively (Table 1). It is noted that all 11 pure lead compounds did not show appreciable cytotoxicity (IC$_{50}$ > 200 μM) against Vero cells (Table 1).

Five lead compounds, **1a-G4**, **1a-G7**, **1b-G1**, **1b-G2**, and **2b-1**, were also assayed for their activities against clinical isolates of *Mtb* strains W210,[26] NHN20,[26] NHN335-2 (isoniazid-resistant, KasA G269S mutation),[27] NHN382

Table 1. Antimicrobial Activities of Selected Trisubstituted Benzimidazoles against Drug-Sensitive and Drug-Resistant Strains of *Mtb*[a]

1a-G1~8 (R^1 = R^2 = Et)
1b-G1,2 (NR^{1}R^2 = pyrrolidine)

2b-1
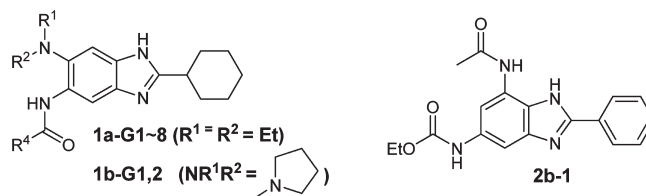
Entry	Benzimidazole	R$_4$	MIC$_{99}$ (µM) *Mtb* strains						Cytotoxicity (IC$_{50}$ µM) Vero cells
			H37Rv	W210	NHN20	NHN335	NHN382	TN587	
1	1a-G1		7.9						>400
2	1a-G2		4.3						>400
3	1a-G3		7.4						>400
4	1a-G4		4.2	4.2	4.2	4.2	4.2	4.2	>400
5	1a-G5		14.1						>400
6	1a-G6		15.1						>400
7	1a-G7		2.0	4.0	4.0	4.0	2.0	4.0	>400
8	1a-G8		3.8						>400
9	1b-G1		1.0	1.0	1.0	1.0	1.0	1.0	>200
10	1b-G2		3.7	3.7	3.7	3.7	3.7	3.7	>200
11	2b-1	Me	2.3	4.6	2.3	2.3	2.3	2.3	>200

[a] *Mtb* H37Rv is a standard drug sensitive strain. *Mtb* W210, NHN 20, NHN335, NHN382, and TN587 are clinical strains with differing drug resistant profiles.

(isoniazide-resistant, Kat G 315T mutation),[26] and TN587 (isoniazide-resistant, KatG S315T mutation),[26] which showed no difference between the drug-sensitive and drug-resistant strains, as anticipated, exhibiting excellent MIC values in the range of 0.39−1.56 µg/mL (1−4.6 µM). These compounds have been advanced to the in vivo rapid model assay in mice.

FtsZ polymerization assay[28] was carried out to validate the hypothesis that these lead compounds exhibit antibacterial activity by interacting with FtsZ. Three benzimidazoles, selected from the 11 lead compounds shown in Table 1, have been evaluated for their ability to inhibit the polymerization of the wild-type FtsZ. **1a-G1** (MIC = 7.9 µM) inhibited FtsZ polymerization in a dose-dependent manner, and ~80% inhibition was achieved at 10 µM (FtsZ concentration of 15 µM) (Figure 3b). A similar result was obtained for **1a-G7** (MIC = 2 µM) (Figure 3a). **1a-G1** and **1a-G7** inhibited FtsZ polymerization with IC$_{50}$ values of 6.21 and 7.69 µM, respectively. **1a-G4** (MIC 4.2 µM), showed ~45% inhibition at 10 µM (Figure 3c).

The assembly and disassembly of FtsZ protein have been shown to be GTP dependent. Since FtsZ has GTPase activity, the Malachite Green assay[29] was performed to monitor the amount of inorganic phosphate (Pi) released upon treatment of *Mtb* FtsZ with two lead compounds, **1a-G4** and **1a-G7**. On treatment of *Mtb* FtsZ with these two compounds, an enhancement in GTPase activity was observed (Figure 4). This unique behavior is analogous to the effect that curcumin exhibited on recombinant *E.coli* FtsZ.[28] Enhancement in the GTPase activity together with the fact that these compounds inhibit polymerization of *Mtb* FtsZ (Figure 3) leads us to conclude that the increased GTPase activity causes the instability of the *Mtb* FtsZ polymer. As a result of the instability, *Mtb* FtsZ is unable to polymerize normally, leading to the efficient inhibition of the formation of sizable *Mtb* FtsZ polymers and filaments.

To further investigate the effect of the hit compounds on polymerization of the FtsZ protein, transmission electron microscopy (TEM) imaging of the treated and untreated *Mtb* FtsZ protein was carried out. *Mtb* FtsZ (5 µM) polymerized in the presence of GTP (25 µM) was diluted 5 times with polymerization buffer and immediately transferred onto a carbon coated copper-mesh grid for TEM imaging. *Mtb* FtsZ protein treated with GTP and 40 and 80 µM **1a-G7** were visualized (Figure 5). The protein treated with colchicine, which is
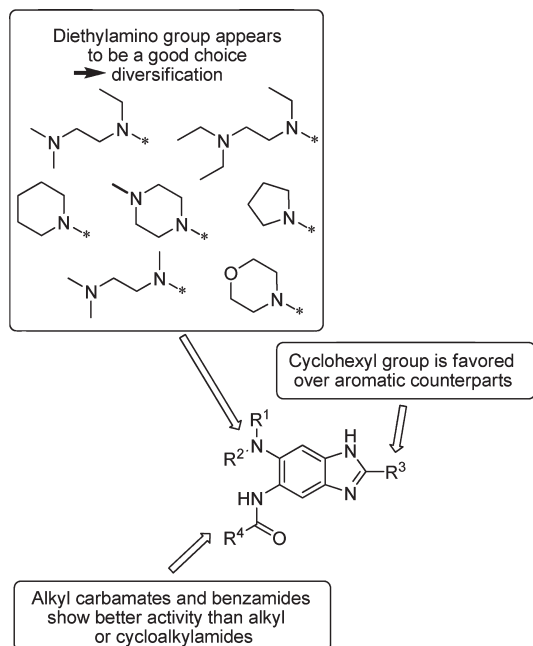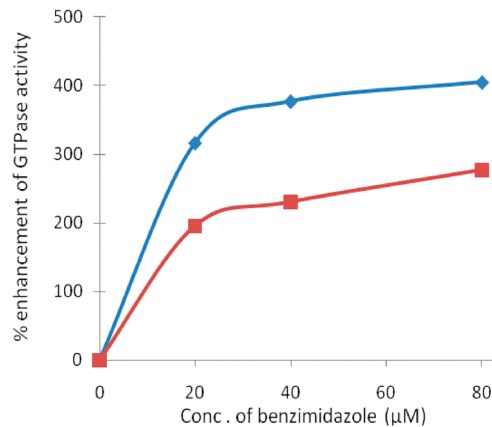
Figure 2. Preliminary SAR of 2,5,6-trisubstituted benzimidazole hit compounds **1a**.
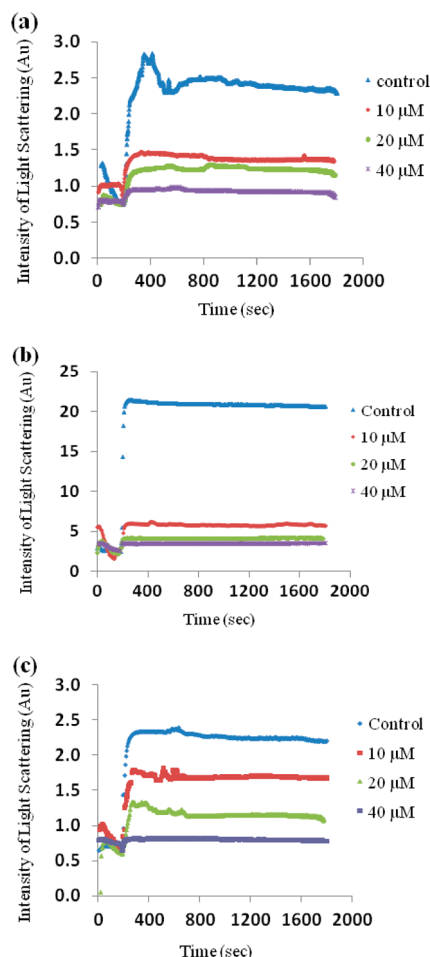
Figure 3. Inhibition of FtsZ polymerization by (a) **1a-G7**, (b) **1a-G1**, and (c) **1a-G4**.

known to inhibit FtsZ polymerization,[13] was used as a reference in this set of experiments (Figure 5F,G). As anticipated,

Figure 4. Enhancement of GTPase activity of FtsZ by lead benzimidazoles **1a-G4** (red) and **1a-G7** (blue).

there was a considerable reduction in the extent of FtsZ protofilament formation upon treatment with **1a-G7** compared to the control experiment. At 40 μM **1a-G7**, the density of *Mtb* FtsZ protofilaments was substantially reduced (Figure 5B,C). Furthermore, the protofilaments were short and very thin. At 80 μM, the formation of protofilaments was drastically reduced and only numerous tiny aggregates were formed (Figure 5D,E). In sharp contrast, the *Mtb* FtsZ protein treated with a high concentration (200 μM) of colchicine showed decreased and thinner protofilaments (Figure 5G,H) but with more or less similar morphology compared with that of GTP-initiated polymerization and protofilaments (Figure 5A,B). These results clearly indicate the highly efficient inhibition of *Mtb* FtsZ assembly by **1a-G7** in a dose-dependent manner with a novel mechanism of action.

Visualization of bacteria treated with 2 × MIC and 4 × MIC **1a-G7** for 2 days using scanning electron microscopy (SEM) revealed altered cell division lengths and aberrant division indicative of the inhibition of FtsZ assembly and cell division (Figure 6). Specifically, cell division and elongation were inhibited in a dose dependent manner resulting in shorter bacterial cells with increased circumferences and altered polar caps. The observed altered bacterial morphology upon exposure to **1a-G7** is thought to result from inhibition of FtsZ leading to disruption in septum formation and recruitment of septum associated proteins involved in later steps of division and septum resolution.

Conclusions

We have created a library of novel trisubstituted benzimidazoles through rational drug design. As Table 1 shows, a good number of these compounds exhibited promising MIC values in the range of 0.5−6.1 μg/mL (1.0−15 μM) for their antibacterial activity against *Mtb* H37Rv strain. Moreover, **1b-G4**, **1b-G7**, **1b-G1**, **1b-G2**, and **2a-1** were also found to exhibit excellent activity against clinical *Mtb* strains W210, NHN20, NHN335, NHN382, and TN587, with different drug-resistance profiles. All lead compounds do not show appreciable cytotoxicity (IC$_{50}$ > 200 μM) against Vero cells. The standard light scattering assay to assess the effect of these compounds on the polymerization of FtsZ clearly showed the inhibition of FtsZ assembly in a dose dependent manner. As the duration of steady state of FtsZ polymer is dependent on the rate of GTP hydrolysis, the effect of lead compounds **1a-G4** and **1a-G7** on GTPase activity was examined. Unexpectedly, instead of
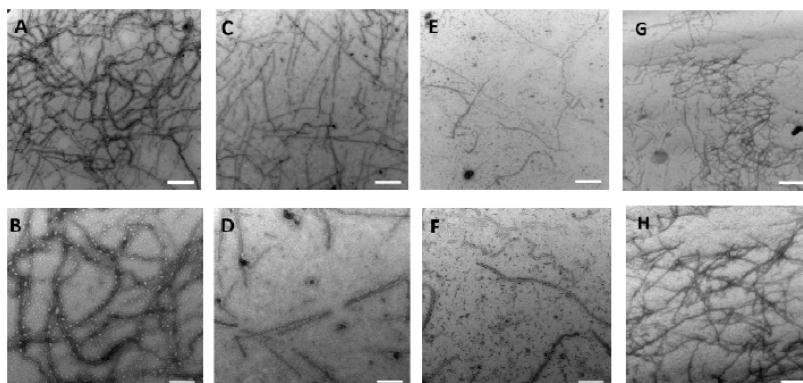
Figure 5. Transmission electron microscope (TEM) images of FtsZ. FtsZ (5 μM) was polymerized by GTP in the absence (A, B) and presence of **1a-G7** at 40 μM (C, D) and 80 μM (E, F). TEM images of the inhibition of FtsZ polymerization in the presence of colchicine at 200 μM (G, H) are also shown for comparison. Images A, C, E, G are at 30000× magnification (scale bar 500 nm), and images B, D, F, H are at 68000× magnification (scale bar 200 nm).
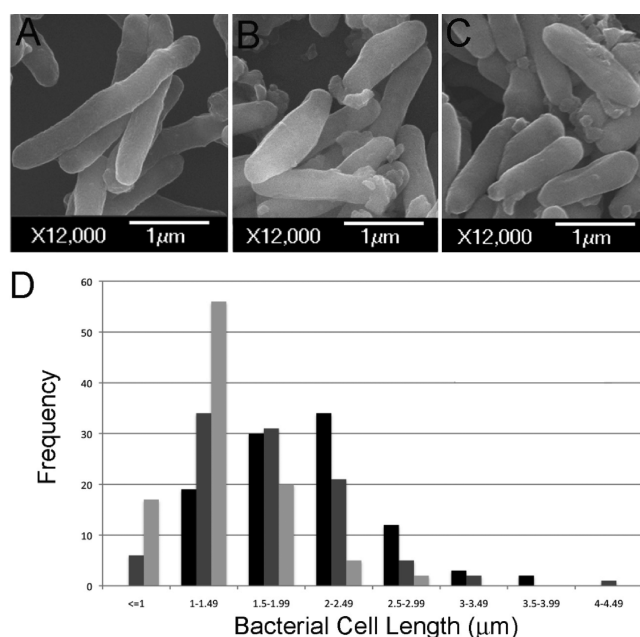
Figure 6. SEM of *Mtb* cells treated with **1a-7** (20000×): (A) control; (B) 2 × MIC; (C) 4 × MIC; (D) distribution of bacterial cell length, showing control (black), 2 × MIC (gray), 4 × MIC (light gray).

inhibiting, these compounds enhanced the GTPase activity of *Mtb* FtsZ by 3- to 4-fold. The result strongly suggests that the increased GTPase activity destabilizes FtsZ polymer, leading to efficient inhibition of FtsZ polymerization and filament formation. The effect of **1a-G7** on FtsZ polymerization was examined by TEM, which revealed an impressive dose-dependent inhibition of Mtb FtsZ assembly and a dramatic suppression of FtsZ protofilament formation at higher concentration of **1a-G7**. The SEM images of *Mtb* cells treated with **1a-G7** showed the absence of septum formation and shorter bacterial cells with increased circumferences and altered polar caps. The unique bacterial morphology indicates that the disruption of septum formation by **1a-G7** may recruit other septum associated proteins involved in later steps of division and septum resolution. The TEM and SEM analyses strongly suggest that **1a-G7** and very likely other lead benzimidazoles have a novel mechanism of action on the inhibition of *Mtb* FtsZ assembly and Z-ring formation. Further optimization and in vivo

evaluation of these highly promising lead compounds are actively underway in these laboratories.

Experimental Section

Methods. ^{1}H and ^{13}C NMR spectra were measured on a Varian 300, 400, or 500 MHz NMR spectrometer. Melting points were measured on a Thomas-Hoover capillary melting point apparatus and are uncorrected. TLC was performed on Merck DC Alufolien with Kieselgel 60F-254, and column chromatography was carried out on silica gel 60 (Merck, 230–400 mesh ASTM). High-resolution mass spectra were obtained from Mass Spectrometry Laboratory, University of Illinois at Urbana—Champaign, Urbana, IL. Purity was determined by an Agilent 1100 series HPLC assembly. Two analytical conditions were used and noted as a part of the characterization data for resynthesized compounds. HPLC1: Luna PFP, 3 μm, 100 Å (pore size), 3.0 mm × 150 mm column, solvent A of H_2O/ACN, 95:5 (20 mM ammonium acetate, pH 6.5), solvent B of H_2O/ACN, 5:95 (20 mM ammonium acetate, pH 6.5), temperature of 30 °C, flow rate of 0.6 mL/min, $t = 0$–13.5 min, gradient of 15–90% solvent B. HPLC2: Kinetex PFP, 2.6 μm, 100 Å (pore size), 4.6 mm × 100 mm column, solvent A of H_2O/ACN, 95:5 (25 mM ammonium acetate, pH 6.5), solvent B of H_2O/ACN, 5:95 (25 mM ammonium acetate, pH 6.5), temperature of 25 °C, flow rate of 1.0 mL/min, $t = 0$–15 min, gradient of 20–95% solvent B. SensoLyte MG phosphate assay kit from Anaspec was used for Malachite Green assay. Light scattering assays were performed using a Fluorolog fluorimeter from ISA. Scanning electron micrographs were obtained with a JEOL JSM-6500F scanning electron microscope. FEI Tecnai12 BioTwinG transmission electron microscope with an AMT XR-60 CCD digital camera system was used to acquire transmission electron microscopy images.

Materials. BL21(DE3)pLysS cells, His-Bind protein purification resin, and the buffers were purchased from Novagen. BCA kit for protein concentration determination was purchased from Sigma. Buffer salts (reagent grade or better), solvents (HPLC grade or better), and all the other chemicals were purchased from Fisher Scientific Co. (Pittsburgh, PA). The chemicals were purchased from Aldrich Co., Synquest Inc., and Sigma and purified before use by standard methods. Tetrahydrofuran was freshly distilled from sodium metal and benzophenone. Dichloromethane was also distilled immediately prior to use under nitrogen from calcium hydride. Aminomethylated polystyrene resin EHL (200–400 mesh) 2% DVB was purchased from Novagenbiochem.

Chemical Synthesis. Novel 2,5,6-trisubstituted benzimidazoles **1** and 2,5,7-trisubstituted benzimidazoles were synthesized in accordance with the general procedures illustrated in

Schemes 1 and 2. The detailed procedures for the syntheses of intermediates **4**, **5**, **6**, **8**, **9**, and **10** as well as their characterization data are described in the Supporting Information.

General Procedure for the Synthesis of the Libraries of Trisubstituted Benzimidazoles 1 and 2. 5-Aminobenzimidazole **6** or 7-aminobenzimidazole **10** (0.005 mmol) was dissolved in dichloromethane and transferred into a 96-well plate. To these wells were added 33 different acyl chlorides (1.1 equiv) or alkyl chloroformates (1 equiv), and they were reacted overnight on a shaker. Aminomethylated polystyrene resin EHL (200−400 mesh) 2% DVB (10 equiv) was added to scavenge excess or unreacted acyl chlorides or alkyl chloroformates. After reacting overnight using the shaker, the resin was filtered to provide a library of trisubstituted benzimidazoles **1** or **2**. The product in each well was analyzed by LC−MS/UV for purity and confirmation of the structure. The purity was in the range of 80−90%.

General Procedure for the Synthesis of Analytically Pure Trisubstituted Benzimidazoles 1 and 2. A typical procedure is described for the synthesis of 5-butoxycarbonylamino-2-cyclohexyl-6-*N,N*-diethylamino-1*H*-benzo[*d*]imidazole (**1a-G7**).

To a solution of 2-cyclohexyl-5-*N,N*-diethylamino-6-aminobenzimidazole (**6a-G**) (486 mg, 1.71 mmol) in dichloromethane (20 mL) was added a solution of *N*-butoxycarbonyloxysuccinimide (340 mg, 1.71 mmol) in dichloromethane (20 mL) dropwise at room temperature. After the addition, the reaction mixture was stirred at room temperature overnight. After the completion of the reaction, the reaction mixture was concentrated. The crude was purified via flash chromatography on silica gel (gradient 20−40% EtOAc/hexanes) to give **1a-G7** as a white solid (336 mg, 51% yield): mp 171−172 °C; ^{1}H NMR (500 MHz, CDCl$_3$) δ 0.91 (t, 6 H, *J* = 7.2 Hz), 0.96 (t, 3 H, *J* = 7.5 Hz), 1.23−1.46 (m, 5 H), 1.57−1.72 (m, 5 H), 1.81 (m, 2 H), 2.07 (m, 2 H), 2.85 (m, 1 H), 2.92 (q, 4 H, *J* = 7.2 Hz), 4.19 (t, 2 H, *J* = 6.5 Hz), 7.46 (s, 1 H), 8.24 (s, 1 H), 8.51 (s, 1 H); ^{13}C NMR (125 MHz, CDCl$_3$) δ 12.72, 13.75, 19.11, 25.81, 26.02, 31.07, 31.78, 38.46, 50.43, 64.87, 98.88, 107.3, 113.3, 131.2, 132.2, 134.3, 138.5, 154.1, 158.8; HRMS (FAB) *m/z* calcd for C$_{22}$H$_{34}$N$_4$O$_2$H$^+$: 387.2763. Found: 387.2760 (Δ = 0.8 ppm). HPLC(2): 10.6 min, purity >99%.

In a similar manner, other lead benzimidazoles were synthesized and characterized.

5-Benzamido-2-cyclohexyl-6-*N,N*-diethylamino-1*H*-benzo[*d*]imidazole (1a-G1). White solid; 74% yield; mp 180−181 °C; ^{1}H NMR (400 MHz, CDCl$_3$) δ 0.97 (t, 6 H, *J* = 7.2 Hz), 1.16 (m, 3 H), 1.65 (m, 5 H), 1.98 (m, 2 H), 2.71 (m, 1 H), 3.03 (m, 4 H, *J* = 6.8 Hz), 7.57 (m, 4 H), 7.98 (d, 2 H, *J* = 6.2 Hz), 8.97 (s, 1 H),10.4 (s, 1 H); ^{13}C NMR (100 MHz, CDCl$_3$) δ 13.09, 21.48, 25.64, 25.91, 31.73, 38.40, 50.77, 100.9, 113.1, 126.9, 129.5, 131.6, 132.7, 135.15, 139.5, 159.8, 165.1; HRMS (FAB) *m/z* calcd for C$_{24}$H$_{30}$N$_4$OH$^+$: 391.2486. Found: 391.2498 (Δ = −3.1 ppm). HPLC(2): 9.50 min, purity >99%.

2-Cyclohexyl-6-*N,N*-diethylamino-5-propoxycarbonylamino-1*H*-benzo[*d*]imidazole (1a-G2). White solid; 63% yield; mp 80−181 °C; ^{1}H NMR (300 MHz, CDCl$_3$) δ 0.92 (t, 6 H, *J* = 7.2 Hz), 0.99 (t, 3 H, *J* = 7.5 Hz), 1.25−1.41 (m, 4 H), 1.60−1.76 (m, 5 H), 1.86 (m, 2 H), 2.10 (m, 2 H), 2.87 (m, 1 H), 2.92 (q, 4 H, *J* = 7.2 Hz), 4.14 (t, 2 H, *J* = 6.6 Hz), 7.47 (s, 1 H), 8.23 (s, 1 H), 8.51 (s, 1 H); ^{13}C NMR (125 MHz, CDCl$_3$) δ 10.28, 12.67, 22.28, 25.71, 25.96, 31.75, 38.44, 50.38, 66.56, 100.0, 112.0, 132.1, 132.4, 134.3, 136.92, 154.1, 159.0; HRMS (FAB) *m/z* calcd for C$_{21}$H$_{32}$N$_4$O$_2$H$^+$: 373.2601. Found: 373.2604 (Δ = −0.8 ppm). HPLC(2): 9.98 min, purity >99%.

2-Cyclohexyl-6-*N,N*-diethylamino-5-(4-methoxybenzamido)-1*H*-benzo[*d*]imidazole (1a-G3). White solid; 79%; mp 198−199 °C; ^{1}H NMR (400 MHz, CDCl$_3$) δ 0.97 (t, 6 H, *J* = 7.2 Hz), 1.16 (m, 3 H), 1.53−1.68 (m, 5 H), 1.98 (m, 2 H), 2.71 (m, 1 H), 3.02 (q, 4 H, *J* = 7.2 Hz), 3.9 (s, 3 H), 7.05 (d, 2 H, *J* = 8.8 Hz), 7.55 (s, 1 H), 7.95 (d, 2 H, *J* = 8.8 Hz), 8.95 (s, 1 H), 10.32 (s, 1 H); ^{13}C NMR (100 MHz, CDCl$_3$) δ 13.36, 25.85, 26.18, 31.96, 38.67, 51.02, 55.75, 101.2, 113.2, 114.2, 127.9, 128.8, 129.0, 132.1, 139.3, 135.2, 160.0,

162.6, 164.9; HRMS (FAB) *m/z* calcd for C$_{25}$H$_{32}$N$_4$O$_2$H$^+$: 421.2601. Found: 421.2604 (Δ = −0.7 ppm). HPLC(2): 9.5 min, purity >99%.

5-But-3-enoxycarbonylamino-2-cyclohexyl-6-*N,N*-diethylamino-1*H*-benzo[*d*]imidazole (1a-G4). White solid; 51% yield; mp 143−145 °C; ^{1}H NMR (500 MHz, CDCl$_3$) δ 0.91 (t, *J* = 7 Hz, 6 H), 1.16−1.31 (m, 3 H), 1.56−1.66 (m, 3 H), 1.77 (d, 2 H, *J* = 13.5 Hz), 2.04 (d, 2 H, *J* = 12.5 Hz), 2.47 (t, 2 H, *J* = 6.5 Hz), 2.83 (m, 1 H), 2.88 (q, 4 H, *J* = 7.5 Hz), 4.23 (t, 2 H, *J* = 7 Hz), 5.11 (m, 2 H), 5.84 (m, 1 H), 7.41 (s, 1 H), 8.24 (s, 1 H), 8.52 (s, 1 H); ^{13}C NMR (125 MHz, CDCl$_3$) δ 12.66, 25.72, 25.96, 31.76, 33.47, 50.39, 63.98, 99.97, 112.1, 117.1, 131.9, 132.0, 131.9, 133.9, 134.3, 137.3, 153.9, 159.2; HRMS (FAB) *m/z* calcd for C$_{22}$H$_{32}$N$_4$O$_2$H$^+$: 385.2604. Found: 385.2604 (Δ = 0.0 ppm). HPLC(2): 10.1 min, purity >99%.

5-(4-Chlorobenzamido)-2-cyclohexyl-6-*N,N*-diethylamino-1*H*-benzo[*d*]imidazole (1a-G5). White solid; 64% yield; mp 216−217 °C (turned brown); ^{1}H NMR (400 MHz, CDCl$_3$) δ 0.96 (t, 6 H, *J* = 7.2 Hz), 1.21−1.32 (m, 2 H), 1.59−1.81 (m, 5 H), 2.08 (m, 2 H), 2.79 (m, 1 H), 3.02 (q, 4 H, *J* = 7.2 Hz), 7.50 (d, 2 H, *J* = 6.8 Hz), 7.58 (s, 1 H), 7.88 (d, 2 H, *J* = 8.8 Hz), 8.82 (s, 1 H),10.31 (s, 1 H); ^{13}C NMR (125 MHz, CDCl$_3$) δ 13.12, 25.75, 25.97, 29.69, 31.76, 38.47, 50.78, 100.5, 113.6, 128.3, 129.1, 131.3, 131.8, 133.9, 135.2, 137.9, 139.6, 159.5, 163.7; HRMS (FAB) *m/z* calcd for C$_{24}$H$_{29}$N$_4$OClH$^+$: 425.2108. Found: 425.2108 (Δ = −0.0 ppm). HPLC(2): 10.5 min, purity >99%.

2-Cyclohexyl-6-*N,N*-diethylamino-5-(4-methylbenzamido)-1*H*-benzo[*d*]imidazole (1a-G6). White solid; 65% yield; mp 183−184 °C; ^{1}H NMR (300 MHz, CDCl$_3$) δ 0.97 (t, 6 H, *J* = 6 Hz), 1.2 (m, 3 H), 1.58−1.78 (m, 5 H), 2.06 (m, 2 H), 2.45 (s, 3 H), 2.76 (m, 1 H), 3.03 (q, 4 H, *J* = 7.2 Hz), 7.34 (d, 2 H, *J* = 8.4 Hz), 7.59 (s, 1 H), 7.87 (d, 2 H, *J* = 8.1 Hz), 8.91 (s, 1 H), 10.31 (s, 1 H); ^{13}C NMR (100 MHz, CDCl$_3$) δ 13.09, 21.48, 25.63, 25.92, 31.72, 38.40, 50.75, 100.9, 113.1, 126.8, 129.6, 131.8, 132.7, 135.0, 139.4, 142.1, 159.8, 165.1; HRMS (FAB) *m/z* calcd for C$_{25}$H$_{32}$N$_4$OH$^+$: 405.2654. Found: 405.2654 (Δ = −0.0 ppm). HPLC(2): 10.1 min, purity >99%.

Benzyloxycarbonylamino-2-cyclohexyl-6-*N,N*-diethylamino-1*H*-benzo[*d*]imidazole (1a-G8). White solid; 61% yield; mp 208−209 °C; ^{1}H NMR (300 MHz, CDCl$_3$) δ 0.90 (t, 6 H, *J* = 7.2 Hz), 1.38 (m, 4 H), 1.84−1.62 (m, 5 H), 2.11 (m, 2 H), 2.84 (m, 1 H), 2.91 (q, 4 H, *J* = 7.2 Hz), 5.22 (s, 2 H), 7.45−7.35 (m, 5 H), 8.25 (s, 1 H), 8.61 (s, 1 H); ^{13}C NMR (125 MHz, CDCl$_3$) δ 12.62, 25.77, 25.97, 31.77, 38.46, 50.41, 66.68, 99.02, 113.2, 128.1, 128.5, 131.3, 132.0, 134.2, 136.3, 138.2, 153.7, 159.0; HRMS (FAB) *m/z* calcd for C$_{25}$H$_{32}$N$_4$O$_2$H$^+$: 421.2601. Found: 421.2604 (Δ = −0.5 ppm). HPLC(2): 10.7 min, purity >99%.

5-Butoxycarbonylamino-2-cyclohexyl-6-(pyrrolidin-1-yl)-1*H*-benzo[*d*]imidazole (1b-G1). White solid; 80% yield; mp 128−129 °C; ^{1}H NMR (500 MHz, CDCl$_3$) δ 0.94 (t, 3 H, *J* = 6.5 Hz), 1.26−1.19 (m, 5 H), 1.73−1.55 (m, 7 H), 1.92 (bs, 4 H), 2.00 (m, 2 H), 2.76 (m, 1 H), 2.93 (bs, 4 H), 4.18 (t, *J* = 6.5 Hz, 2 H), 7.40 (s, 1 H), 7.95 (s, 1 H), 8.17 (s,1 H); ^{13}C NMR (125 MHz, CDCl$_3$) δ 13.68, 19.03, 24.24, 25.71, 25.94,30.99, 31.75, 38.45, 53.41, 64.90, 101.3, 109.80, 129.3, 131.8, 135.6, 137.5, 154.3, 159.1. HRMS (FAB) *m/z* calcd for C$_{22}$H$_{32}$N$_4$O$_2$H$^+$: 385.2594. Found: 385.2604 (Δ = −1.1 ppm). HPLC(2): 10 min, purity >99%.

5-Benzyloxycarbonylamino-2-cyclohexyl-6-(pyrrolidin-1-yl)-1*H*-benzo[*d*]imidazole (1b-G2). White solid; 68% yield; mp 86−87 °C; ^{1}H NMR (500 MHz, CDCl$_3$) δ 1.21−1.28 (m, 4 H), 1.59−1.65 (m, 4 H), 1.76 (m, 2 H), 1.91 (s, 4 H), 2.04 (d, 2H, *J* = 12.5 Hz), 2.82 (m, 1 H), 2.93 (s, 4 H), 5.22 (s, 2 H), 7.34−7.48 (m, 5 H aromatic), 8.08 (s, 1 H), 8.22 (s, 1 H); ^{13}C NMR (125 MHz, CDCl$_3$) δ 24.29, 25.69, 25.91, 31.72, 38.31, 53.54, 66.75, 101.5, 108.7, 128.1, 128.5, 129.6, 131.9, 136.0, 136.2, 153.8, 158.9. HRMS (FAB) *m/z* calcd for C$_{25}$H$_{30}$N$_4$O$_2$H$^+$: 419.2448. Found: 419.2447 (Δ = 0.2 ppm). HPLC(2): 10.1 min, purity >99%.

7-Acetylamino-5-ethoxycarbonylamino-2-phenyl-1*H*-benzo[*d*]imidazole (2a-1). White solid; 84% yield: mp 158−160 °C;

^{1}H NMR (400 MHz, CD$_3$OD) δ 1.32 (t, J = 7.2 Hz, 3H), 2.26 (s, 3H), 4.20 (q, J = 7.2 Hz, 2H), 7.54 (m, 3H), 7.69 (bs, 1H), 7.79 (bs, 1H), 8.05 (m, 2H); ^{13}C NMR (100 MHz, DMSO) δ 14.59, 23.99, 59.92, 96.14, 105.46, 126.18, 128.87, 129.16, 129.48, 130.08, 131.28, 131.82, 135.21, 149.61, 153.74, 168.61. HRMS (FAB) m/z calcd for C$_{18}$H$_{18}$N$_4$O$_3$H$^+$: 339.1450. Found: 339.1457 (Δ = −2.1 ppm). HPLC(2): 4.95 min, purity > 99%.

Bacterial Strains and Growth. H37Rv, the drug sensitive laboratory strain of *Mtb*, and clinical *Mtb* strains W210, NHN20, HN355, NHN382, and TN587 exhibit different resistant profiles to isoniazid and rifampicin.[8,27] For evaluation of drug sensitivity all strains were grown in 7H9 media containing 10% oleic acid/albumin/catalase ; /catalase (OADC) enrichment and 0.05% Tween-80 and assessed at mid log phase growth.

Antibacterial Activity. The minimum inhibitory concentration (MIC) was determined by the microplate Alamar Blue assay (MABA) as described previously.[25] Briefly, stock solutions of the compounds were prepared in DMSO and were serially diluted 2-fold in 96-well microtiter plates, and each *Mtb* strain was added to each well to an OD$_{600}$ of 0.005. Plates were incubated for 6 days at 37 °C. Alamar Blue (Invitrogen) was added to the plates, and the plates were incubated for an additional 24 h at 37 °C. Plates were monitored for color change, and MIC$_{99}$ was determined in triplicate.

Cytoxicity Assay. The cytotoxicity of the compounds was tested against VERO cells. Epithelial cells from the kidneys of the African Green Monkey were used to start the VERO cell line. Vero cells were grown in L15 media without CO$_2$. Serial 2-fold dilutions of the drugs were prepared in the 96-well microtiter plates. The cells were added to the plates in media containing the appropriate amount of Alamar Blue. The cells were added to a final concentration of 2.5×10^4/well. The plates were incubated for 3 days at 37 °C. The IC$_{50}$ was calculated according to manufacturer directions.

FtsZ Polymerization Inhibitory Assay.[12] The inhibitory activity of lead benzamidazoles for *Mtb* FtsZ polymerization was determined by means of light scattering on a PTI Fluorescence Master system. The 90° light scattering was measured at 30 °C, using excitation and emission wavelength of 400 nm with slit width of 2 nm. The gain was set at 950 V. *Mtb* FtsZ (15 μM) was incubated in the polymerization buffer (50 mM MES, 5 mM MgCl$_2$, 50 mM KCl, pH 6.5) to establish a baseline. Then 5 mM GTP (20 μL) was added to make the final volume 1000 μL in a 1.5 mL cuvette. The light scattering was measured for a period of 30−60 min. When DMSO was used as a solvent for the inhibitor, the control also contained the same amount of DMSO. For inhibition studies, a lead benzimidazole at various concentrations was incubated with the polymerization buffer to establish a baseline. This was followed by addition of FtsZ (15 μM). Once the baseline was stabilized, 5 mM GTP (20 μL) was added to make the final volume 1000 μL in a 1.5 mL cuvette and the light scattering was measured.

GTPase Assay. The amount of inorganic phosphate (Pi) released during the assembly of FtsZ was measured using a standard Malachite Green/ammonium molybdate assay.[29] Briefly, FtsZ protein (10 μM) was incubated without or with a benzimidazole at different concentrations (0, 20, 40, and 80 μM) in polymerization buffer (50 mM MES, 5 mM MgCl$_2$, 50 mM KCl, pH 6.5) at room temperature for 15 min. Then 50 μM GTP was added to the reaction mixture and incubated at 37 °C to start the hydrolysis reaction. After 30 min of incubation, Malachite Green reagent (20% v/v) was added to the reaction mixtures to quench the reaction. The reaction mixtures were centrifuged at 13 000 rpm for 90 s to remove the protein debris. The samples (100 μL) were transferred to a 96-well plate, and the absorbance of each well was measured at 620 nm. The background absorbance was subtracted from all the readings. A phosphate standard curve was prepared using phosphate standard provided with a Malachite Green assay kit (SensoLyte). All the solutions were prepared in polymerization buffer.

Transmission Electron Microscopy (TEM) Analysis. *Mtb* FtsZ (5 μM) was incubated with 40 or 80 μM **1a-G7** in the polymerization buffer (50 mM MES, 5 mM MgCl$_2$, 50 mM KCl, pH 6.5) for 15−20 min. To each solution was added GTP to the final concentration of 25 μM. The resulting solution was incubated at 37 °C for 30 min. The incubated solution was diluted 5 times with the polymerization buffer and immediately transferred to carbon coated 300 mesh formvar copper grid and negatively stained with 1% uranyl acetate. The samples were viewed with a FEI Tecnai12 BioTwinG transmission electron microscope at 80 kV.[19] Digital images were acquired with an AMT XR-60 CCD digital camera system.

Ultrastructural Analysis via Scanning Electron Micrscopy (SEM). *Mtb* H37Rv bacteria were exposed to 2 × MIC and 4 × MIC **1a-G7** for 2 days. The bacteria were prepared for scanning electron microscopy as described by Slayden et al.[8] Briefly, bacteria were prepared for SEM treatment with 2.5% glutaraldehyde in 0.1 M sodium cacodyte (pH 7.2), 5 mM CaCl$_2$, and 5 mM MgCl$_2$ and incubated at room temperature for 1−2 h. The fixed bacteria were harvested by centrifugation and washed in PBS and subjected to 2.5% glutaraldehyde overnight at 4 °C. Final preparation for SEM was achieved by treatment with 1% OsO$_4$ in sodium cacodylate buffer and dehydration in a graded alcohol series. The bacteria were then examined using a JEOL JSM-6500F scanning electron microscope. Bacteria from all treatment groups were measured for their lengths. Size frequency graphs were prepared for each treatment group.

Supporting Information Available: Synthetic procedures and characterization data for new benzimidazole intermediates as well as Mtb FtsZ protein preparation. This material is available free of charge via the Internet at http://pubs.acs.org.

References

(1) World Health Organization. Tuberculosis: Data and Country Profiles. http://www.who.int/tb/country/en/.

(2) Raviglione, M. C. Issues facing TB control (7). Multiple drug-resistant tuberculosis. *Scott. Med. J.* **2000**, *45* (5, Suppl.), 52−55, discussion 56.

(3) Gandhi, N. R.; Moll, A.; Sturm, A. W.; Pawinski, R.; Govender, T.; Lalloo, U.; Zeller, K.; Andrews, J.; Friedland, G. Extensively drug-resistant tuberculosis as a cause of death in patients co-infected with tuberculosis and HIV in a rural area of South Africa. *Lancet* **2006**, *368* (9547), 1575−1580.

(4) Errington, J.; Daniel, R. A.; Scheffers, D.-J. Cytokinesis in bacteria. *Microbiol. Mol. Biol. Rev.* **2003**, *67* (1), 52−65.

(5) Bi, E.; Lutkenhaus, J. FtsZ Ring structure associated with division in *Escherichia coli*. *Nature* **1991**, *354*, 161−164.

(6) Vollmer, W. The prokaryotic cytoskeleton: a putative target for inhibitors and antibiotics? *Appl. Microbiol. Biotechnol.* **2006**, *73* (1), 37−47.

(7) Huang, Q.; Tonge, P. J.; Slayden, R. A.; Kirikae, T.; Ojima, I. FtsZ: a novel target for tuberculosis drug discovery. *Curr. Top. Med. Chem.* (*Sharjah, United Arab Emirates*) **2007**, *7* (5), 527−543.

(8) Slayden, R. A.; Knudson, D. L.; Belisle, J. T. Identification of cell cycle regulators in *Mycobacterium tuberculosis* by inhibition of septum formation and global transcriptional analysis. *Microbiology* (*Reading, U. K.*) **2006**, *152* (6), 1789−1797.

(9) Respicio, L.; Nair, P. A.; Huang, Q.; Burcu, A. B.; Tracz, S.; Truglio, J. J.; Kisker, C.; Raleigh, D. P.; Ojima, I.; Knudson, D. L.; Tonge, P. J.; Slayden, R. A. Characterizing septum inhibition in *Mycobacterium tuberculosis* for novel drug discovery. *Tuberculosis* **2008**, *88*, 420−429.

(10) Nogales, E.; Wang, H. W. Structural mechanisms underlying nucleotide-dependent self-assembly of tubulin and its relatives. *Curr. Opin. Struct. Biol.* **2006**, *16*, 221−229.

(11) Farmer, P.; Bayona, J.; Becerra, M.; Furin, J.; Henry, C.; Hiatt, H.; Kim, J. Y.; Mitnick, C.; Nardell, E.; Shin, S. The dilemma of MDR-TB in the global era. *Int. J. Tuberc. Lung Dis.* **1998**, *2* (11), 869–876.

(12) White, E. L.; Ross, L. J.; Reynolds, R. C.; Seitz, L. E.; Moore, G. D.; Borhani, D. W. Slow polymerization of *Mycobacterium tuberculosis* FtsZ. *J. Bacteriol.* **2000**, *182*, 4028–4034.

(13) White, E. L.; Suling, W. J.; Ross, L. J.; Seitz, L. E.; Reynolds, R. C. 2-Alkoxycarbonylaminopyridines: inhibitors of *Mycobacterium tuberculosis* FtsZ. *J. Antimicrob. Chemother.* **2002**, *50* (1), 111–114.

(14) Reynolds, R. C.; Srivastava, S.; Ross, L. J.; Suling, W. J.; White, E. L. A new 2-carbamoyl pteridine that inhibits mycobacterial FtsZ. *Bioorg. Med. Chem. Lett.* **2004**, *14* (12), 3161–3164.

(15) Margalit, D. N.; Romberg, L.; Mets, R. B.; Hebert, A. M.; Mitchison, T. J.; Kirschner, M. W.; RayChaudhuri, D. Targeting cell division: small-molecule inhibitors of FtsZ GTPase perturb cytokinetic ring assembly and induce bacterial lethality. *Proc. Natl. Acad. Sci. U.S.A.* **2004**, *101* (38), 13969; erratum to document cited in CA141:271048 .

(16) Urgaonkar, S.; La Pierre, H. S.; Meir, I.; Lund, H.; Ray Chaudhuri, D.; Shaw, J. T. Synthesis of antimicrobial natural products targeting FtsZ: (+−)-dichamanetin and (+−)-2‴-hydroxy-5″-benzylisouvarinol-B. *Org. Lett.* **2005**, *7* (25), 5609–5612.

(17) Rai, D.; Singh, J. K.; Roy, N.; Panda, D. Curcumin inhibits FtsZ assembly: an attractive mechanism for its antibacterial activity. *Biochem. J.* **2008**, *410* (1), 147–155.

(18) Domadia, P.; Swarup, S.; Bhunia, A.; Sivaraman, J.; Dasgupta, D. Inhibition of bacterial cell division protein FtsZ by cinnamaldehyde. *Biochem. Pharmacol.* **2007**, *74* (6), 831–840.

(19) Jaiswal, R.; Beuria, T. K.; Mohan, R.; Mahajan, S. K.; Panda, D. Totarol inhibits bacterial cytokinesis by perturbing the assembly dynamics of FtsZ. *Biochemistry* **2007**, *46* (14), 4211–4220.

(20) Stokes, N. R.; Sievers, J.; Barker, S.; Bennett, J. M.; Brown, D. R.; Collins, I.; Errington, V. M.; Foulger, D.; Hall, M.; Halsey, R.; Johnson, H.; Rose, V.; Thomaides, H. B.; Haydon, D. J.; Czaplewski, L. G.; Errington, J. Novel inhibitors of bacterial cytokinesis identified by a cell-based antibiotic screening assay. *J. Biol. Chem.* **2005**, *280* (48), 39709–39715.

(21) Ito, H.; Ura, A.; Oyamada, Y.; Tanitame, A.; Yoshida, H.; Yamada, S.; Wachi, M.; Yamagishi, J.-i. A 4-aminofurazan derivative-A189-inhibits assembly of bacterial cell division protein FtsZ in vitro and in vivo. *Microbiol. Immunol.* **2006**, *50* (10), 759–764.

(22) Paradis-Bleau, C.; Beaumont, M.; Sanschagrin, F.; Voyer, N.; Levesque, R. C. Parallel solid synthesis of inhibitors of the essential cell division FtsZ enzyme as a new potential class of antibacterials. *Bioorg. Med. Chem.* **2007**, *15* (3), 1330–1340.

(23) Huang, Q.; Kirikae, F.; Kirikae, T.; Pepe, A.; Amin, A.; Respicio, L.; Slayden, R. A.; Tonge, P. J.; Ojima, I. Targeting FtsZ for antituberculosis drug discovery: noncytotoxic taxanes as novel antituberculosis agents. *J. Med. Chem.* **2006**, *49* (2), 463–466.

(24) Kumar, K.; Lee, S.-Y.; Zanardi, I.; Slayden, R. A.; Ojima, I., Synthesis and Optimization of a Library of Novel Benzimidazole Leads for Antituberculosis Drug Discovery. Presented at the 234th National Meeting of the American Chemical Society, Boston, MA, United States, August 19−23, 2007; MEDI-205.

(25) Collins, L.; Franzblau, S. G. Microplate Alamar blue assay versus BACTEC 460 system for high-throughput screening of compounds against *Mycobacterium tuberculosis* and *Mycobacterium avium*. *Antimicrob. Agents Chemother.* **1997**, *41* (5), 1004–1009.

(26) Boyne, M. E.; Sullivan, T. J.; amEnde, C. W.; Lu, H.; Gruppo, V.; Heaslip, D.; Amin, A. G.; Chatterjee, D.; Lenaerts, A.; Tonge, P.J.; Slayden, R. A. Targeting fatty acid biosynthesis for the development of novel chemotherapeutics against *Mycobacterium tuberculosis*: evaluation of A-ring-modified diphenyl ethers as high-affinity InhA inhibitors. *Antimicrob. Agents Chemother.* **2007**, *51*, 3562–3567.

(27) Slayden, R. A.; Lee, R. E.; Barry, C. E. Isoniazid effects multiple components of the type II fatty acid synthase system of *Mycobacterium tuberculosis*. *Mol. Microbiol.* **2000**, *38* (3), 514–525.

(28) Mukherjee, A.; Lutkenhaus, J. Analysis of FtsZ assembly by light scattering and determination of the role of divalent metal cations. *J. Bacteriol.* **1999**, *181* (3), 823–832.

(29) Geladopoulos, T. P.; Sotiroudis, T. G.; Evangelopoulos, A. E. A Malachite Green colorimetric assay for protein phosphatase activity. *Anal. Biochem.* **1991**, *192*, 112–116.